DOI: 10.14264/uql.2020.585

Experimental analysis on sediment transport phenomena in channels equipped with inclined side weirs

M. Di Bacco[1], A. R. Scorzini[1] and M. Leopardi[1]
[1] Department of Civil, Environmental and Architectural Engineering
University of L'Aquila
L'Aquila, Italy
E-mail: mario.dibacco@univaq.it

ABSTRACT

Side weirs are particular structures used in hydraulic engineering for flow control in rivers and channels. In movable bed situations, the lateral discharge withdrawal can influence sediment transport processes causing an unexpected functioning of the weir; due to the possible changes in bed morphology, sediments from the main channel can be diverted in the evacuation channel as well. This paper summarizes the results of experimental analyses carried out to study these interactions for inclined weirs, under different hydraulic and geometric conditions. The results show the influence of weir's length and inclination of the crest on the pattern of deposition and erosion zones in the main channel. The analysis of the experimental observations also confirm the validity of the De Marchi's approach for modelling the behavior of inclined side weirs on movable beds. In addition, the predictive capability of a numerical method for estimating the diverted solid discharge from side weirs is tested. The comparison of observed and predicted sediment discharges outflowing from the lateral structure indicates the reliability of the tested method also for inclined side weirs.

Keywords: *side weir, inclined, sediment transport, bed morphology, De Marchi's approach.*

1. INTRODUCTION

Side weirs are diversion devices commonly used in hydraulic engineering to spill out a part of the discharge from the main channel when a design water level is exceeded. The investigation of flow features over side weirs has been the objective of many theoretical and experimental studies since the early 1900s (e.g., Coleman and Smith 1923; De Marchi 1934; Hager 1987; Subramanya and Awasthy 1972; Muslu 2001; Castro-Orgaz and Hager 2012; Maranzoni et al. 2017). Most of the literature assumed a non-erodible channel bed, which is an adequate hypothesis for lateral weirs placed in (artificial) irrigation or drainage channels. Differently, in natural rivers, characterized by a movable bed, sediment transport phenomena may have a significant impact on the hydraulic behavior of side weirs, due to possible morphological bed modifications induced by the presence of the diversion structure. In the last decade, some authors have started to investigate the effect of lateral discharge withdrawal from horizontal side weirs on the evolution of bed morphology: they showed the formation of a local sediment deposit in the downstream section of the weir, which causes an increment of the outflow over the development of the deposition process (Rosier 2007; Rosier et al. 2009, 2010; Paris et al. 2012; Michelazzo et al. 2016).

In this framework, the main objective of the present paper is to further enhance current knowledge on sediment transport phenomena in channels equipped with side weirs, by extending the focus on unconventional inclined-crested geometries (Figure 1) of the diversion device (Aghayari et al. 2009; Wang et al., 2018; Di Bacco et al. 2019).

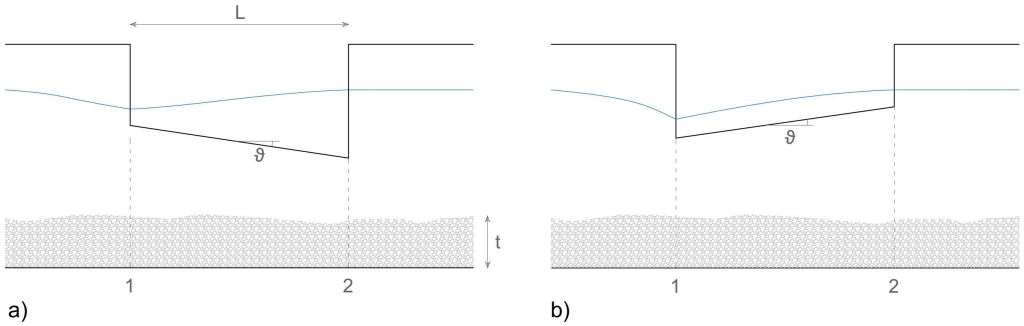

Figure 1. Schematization of inclined side weirs: a) downward configuration; b) upward configuration.

In particular, results of flume experiments carried out in the Laboratory of Hydraulic Structures at the University of L'Aquila are first considered to test the validity of the well-known De Marchi's approach (De Marchi 1934) also for the case of inclined side weirs in presence of movable beds. Then, particular attention is paid to the analysis of the influence of weir length and crest angle on the modifications of bed morphology and on sediment exchange processes between the main channel and the evacuation channel.

2. METHODOLOGY

2.1. Experimental setup and measurements

Experiments were carried out in a 20 cm wide and 17 m long movable bed laboratory flume (thickness of bed layer t ranging between 20 and 30 cm along the main channel), which was sided in the last 5 m by an evacuation channel that was fed by a lateral weir, characterized by different tested geometries. The size of bed material (median diameter d_{50} = 2 mm, specific weight of sediments γ_s = 26.5 kN/m^3) was chosen in order to avoid suspended sediment and to observe only bedload transport. The reference bed configuration was determined in an initial calibration phase (with the side weir completely closed, i.e. no outflow in the lateral channel), by supplying a constant flow rate of 10 l/s until an equilibrium profile was reached (with a resulting average 7÷8‰ slope). Given the length and size of the flume, the presence of a sufficient sediment layer in the upstream reach was continuously monitored, as this part of the experimental channel was considered as feeding tank for the sediment discharge.

The effect of the lateral flow withdrawal on sediment transport was studied for 40 different combinations of hydraulic conditions and geometric configurations of the diversion device; in particular, the following parameters were tested:

- 4 values of the flow discharge in the main channel, Q_1: 7, 8.5, 10 and 11.5 l/s (subcritical flow);
- 5 values of the crest slope of the side weir, ϑ: 3°, 6° (both upward and downward inclinations), including the horizontal case (ϑ = 0°);
- 2 values of the length of the side weir, L: 34.5 cm and 19.5 cm (corresponding to an adimensional length L/B equal to 1.73 and 0.97, respectively, where B is the main channel width).

The duration of the runs was not predetermined, but in each of them it was checked that an equilibrium condition had been attained. This was verified by measuring with a point gauge bed and water elevations in the centerline of the main channel, at four control sections, located at the initial and final ends of the weir, 20 cm upstream from the first one and 50 cm downstream from the second one. Equilibrium was considered to be reached when no differences between two successive measurements, taken at 30-minute intervals, were observed. In this steady condition, the quantity of sediments leaving the main channel (i.e. the solid flow rate derived from the side weir) was measured in a non-intrusive way, by manually intercepting for 60 seconds the flow in the evacuation channel with a suitable net, capable of entrapping the incoming sediments; this material was dried and then weighed. For each experiment, once the main channel had been completely drained, a camera with fixed focus was used to capture numerous images of the final bed configuration. After this operation, channel bed was restored to the reference configuration to be used in the subsequent runs.

2.2. 3D reconstruction of bed morphology

Acquired images were processed in order to reconstruct a 3D view of the bed morphology in the different tested conditions, using the Structure from Motion technique (Westoby et al. 2012; Wu 2013). With this method, the 3D morphologies of the bed were generated from point clouds automatically extracted from sets of multiple overlapping images (Wu 2013). A common reference system was defined for the point clouds, using 9 references points, with known coordinates, adjacent to the channel and easily recognizable in all tests; given the redundancy of the points, it was possible to estimate the error in system repositioning, which was always smaller than 2 mm. Each point cloud was then converted by linear spatial interpolation into a raster with a resolution of 5 mm, representing the digital elevation model (DEM) of the channel bed. In order to avoid errors in the DEM reconstruction due to possible presence of noise in the sampled data, the point clouds were filtered by implementing a two-step algorithm. All the data points with an elevation which differed from the average by more than 8 cm, clearly not belonging to the bed (e.g., sediments occasionally fallen on the floor of the laboratory), were first removed. Then, several alternative filtering methods were examined and the most convincing results were obtained with a median filter modified with an additional condition, as follows: for each point P of the DEM,

characterized by an elevation value z_P, the median elevation z_m of the neighboring points was calculated and compared to z_P; all the points for which the absolute difference $| z_P - z_m |$ was greater than $dx \cdot tan(\Phi)$ - where dx is the spatial resolution of the DEM and Φ is the friction angle of the sediments (estimated equal to 35°) - were eliminated and replaced by z_m.

2.3. Assessment of the validity of De Marchi's approach

De Marchi's (1934) approach, solving the 1D dynamic equation of spatially varied steady flow with non-uniform discharge, is commonly accepted in the design of side weirs. The method is based on the assumption that the specific energy along the weir is constant and that the diverted flow can be estimated by using Poleni's equation for frontal weirs. For horizontal side weirs, the validity of De Marchi's hypothesis has been verified in several experimental investigations, in fixed as wells as movable bed conditions (e.g. Bagheri et al. 2014; Paris et al. 2012); however, no previous investigations have been performed in the case when both movable bed conditions and inclined crest configurations are present. To fill this gap, in this study we extended the analysis proposed by Paris et al. (2012) to inclined side weirs.

The application of De Marchi's hypothesis to upstream and downstream ends (denoted respectively with subscripts 1 and 2) of a lateral weir leads to:

$$z_1 + h_1 + \alpha_1 \frac{Q_1^2}{2g\Omega_1^2} = z_2 + h_2 + \alpha_2 \frac{(Q_1^2 - Q_d^2)}{2g\Omega_2^2} \quad (1)$$

where z_i is the bed elevation, h_i is the water depth, α_i is the Coriolis coefficient (May et al. 2003; Paris et al. 2012), Ω_i is the liquid area ($B_i \cdot h_i$) and Q_1 and Q_d are respectively the flow in the main channel and the diverted flow. The difference in the mean bed elevation $z_1 - z_2$ between the examined cross sections can be expressed as follows (Paris et al. 2012):

$$z_2 - z_1 = k \cdot \Delta \quad (2)$$

where Δ is the measured bottom step height (derived from the analysis of the reconstructed DEM) and k is a reduction coefficient accounting for the 3D features of the bed deformations close to the later weir ($k < 1$), which can be estimated experimentally by means of Eq. (1) as a function of the ratio Q_d/Q_1. To assess the De Marchi's assumption, once k values had been determined, the specific energy at the upstream and downstream ends of the weir were then calculated as:

$$E_1 = h_1 + \alpha_1 \frac{Q_1^2}{2g\Omega_1^2} \quad \text{and} \quad E_2 = k \cdot \Delta + h_2 + \alpha_2 \frac{(Q_1^2 - Q_d^2)}{2g\Omega_2^2} \quad (3)$$

2.4. Analysis of sediment outflow from the side weir

For each experimental configuration, the measured solid discharge outflowing from the side weir in equilibrium conditions (Section 2.1) was compared to that estimated following the approach proposed by Michelazzo et al. (2016) for horizontal side weirs, with the aim of testing its predictive capability. The authors calculated the sediment transport over the side weir as a function of stream power associated with the spilled discharge (Michelazzo et al. 2016), expressed in terms of Van Rijn's sediment transport parameter T (Van Rijn 1984):

$$T = \frac{\tau - \tau_{cr}}{\tau_{cr}} \quad (4)$$

where $\tau = (\tau_x^2 + \tau_y^2)^{1/2}$ is the total bed-shear stress and τ_{cr} is the critical value of bed-shear stress for incipient motion of the sediments. The two components τ_x and τ_y can be defined as:

$$\tau_x(x) = \rho \frac{\sqrt{u(x)^2 + v(x)^2}}{C(x)^2} u(x) \quad ; \quad \tau_y(x) = \rho \frac{\sqrt{u(x)^2 + v(x)^2}}{C(x)^2} v(x) \quad (5)$$

where ρ is water density and $C(x)$ is the adimensional roughness coefficient, while the components of the depth-averaged flow velocities in the main flow direction $u(x)$ and transversal direction $v(x)$ can expressed as:

$$u(x) = \frac{Q_1 - Q_d(x)}{Bh(x)} \quad ; \quad v(x) = \frac{1}{h(x)} \frac{dQ_d(x)}{dx} \quad (6)$$

where $h(x)$ is the water depth elevation, Q_1 and Q_d are, respectively, the total flow in the main channel and the flow diverted from the lateral weir in the equilibrium phase; the last term can be expressed by means of the side-weir equation (De Marchi 1934), which can be solved by using the measured water surface profile over the side

weir $y(x)$ and the experimentally derived De Marchi coefficient C_M. In this way, with the set of previous equations, it is possible estimate $u(x)$, $v(x)$, τ_x and τ_y and then T, in which τ_{cr} is related to the sediment size by means of Van Rijn's equation (Van Rijn 1984). Finally, the diverted volumetric sediment discharge per unit length of the side weir, to be compared to the measured one, can be expressed as (Bagnold 1966):

$$q_{sb} = \frac{T \cdot \tau_y \cdot v(x)}{\gamma_s} \tag{7}$$

with γ_s indicating the specific weight of the sediments.

3. RESULTS AND DISCUSSION

3.1. Evolution of bed morphology due to discharge withdrawal

Figure 2 shows observed longitudinal bed profiles in equilibrium conditions extracted from the reconstructed DEMs, in three sections located, respectively, in proximity of the side weir (y=5 mm in the transversal direction), at the centerline of the main channel (y=10 cm) and near the channel wall opposite to the diversion structure (y=18 cm). The figure refers to the same inflowing discharge Q_1=11.5 l/s and two lengths of the side weir, L_1=34.5 cm (left) and L_2=19.5 cm (right) for all tested crest angles; reference bed configuration (blue line) is reported as well for comparison purposes. The part of Figure 2 related to the longer weir length L_1 indicates systematic erosion downstream from the weir in the closest section to the structure (y = 5 mm), over a length extending over a distance ranging from 50 to 60 cm, depending on crest angle ϑ; this configuration was due to the impact of the flow drawn by the spillway against the downstream wall, at the stagnation point (Neary et al. 1999).

While for upward geometries ($\vartheta > 0°$) the channel area affected by erosion was very limited and confined in proximity to the weir section, for downward and horizontal configurations ($\vartheta \leq 0°$), an erosion band affecting the entire channel section (over a length similar to L_1) was noted downstream from the structure; this erosion then changed to a deposition zone in the terminal part of the channel, with an approximately, although not always symmetrical, sinusoidal profile. Maximum scour depths (about 6 cm near the diversion section and diminishing to 4 cm near the opposite wall) were measured for downward geometries of the lateral weir, independently of ϑ values; the magnitude of this scour depth was clearly found to be a function of the flow Q_1, as depicted in Figure 3, which shows measured longitudinal bed profiles at y=10 cm for the two tested negative crest angles under increasing upstream flow values.

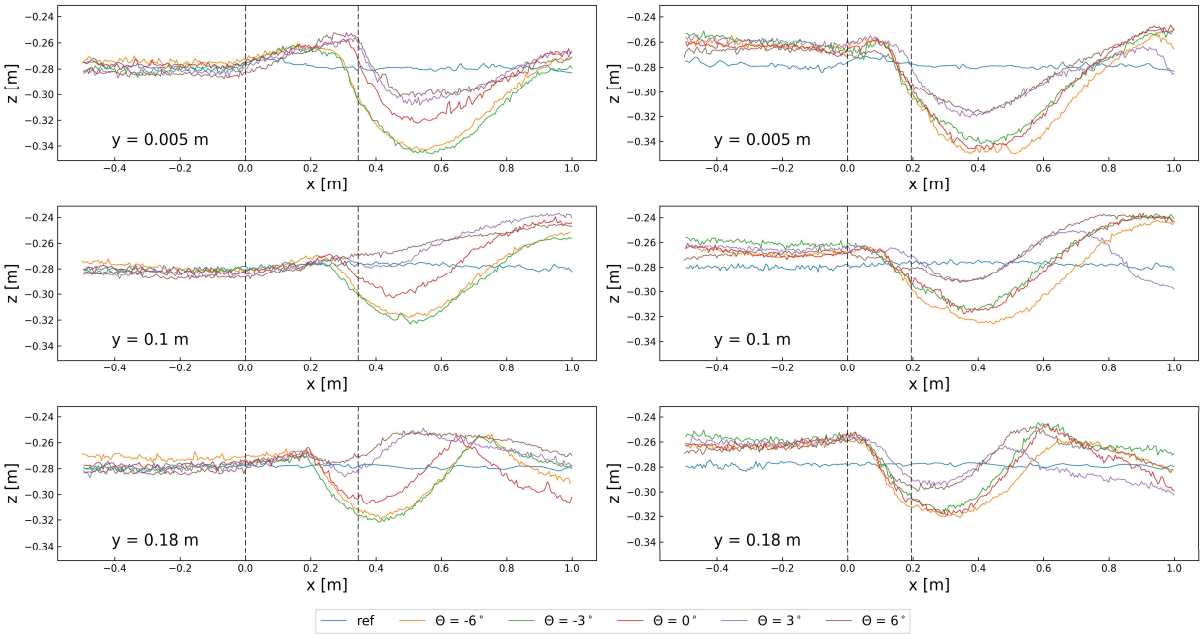

Figure 2. Observed longitudinal bed profiles at different transversal sections for tested crest slopes of the side weir (left: length of the weir L_1=34.5 cm; right: L_2=19.5 cm; weir position is indicated with the dashed lines).

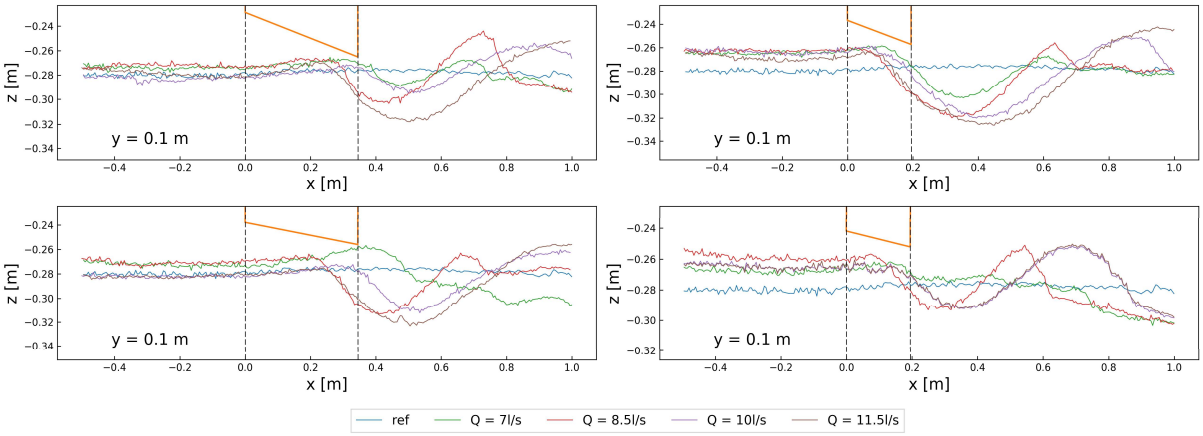

Figure 3. Observed longitudinal bed profiles for different flow values at the cross-section located in y=10 cm for ϑ = -6° (top panel) and ϑ = -3° (bottom panel).

A different behavior was observed for upward configurations, which induced the formation of a deposition zone extending over large part of the channel, with increasing depth starting from the downstream end of the weir (maximum values of about 4 cm at the centerline section and diminishing to about 2 cm at y=18 cm). Furthermore, deposition was always detected in proximity of the inlet of the lateral weir, with more pronounced profiles for ϑ>0°; this pattern almost disappeared in the transversal direction.

For the shorter weir length L_2, Figure 2 shows the formation of a scour hole downstream from the end of the structure, extending over the whole channel width for a distance ranging from 20-40 cm at y=18 cm to 50-60 cm at y=5 mm, depending on the inclination of the weir crest. Similarly to the previous case, this erosion zone was followed by a dune formation in the downstream part of the channel. Deposition at weir section was less marked than that observed in previous cases, while an extended sediment deposit of about 1.4 cm in the upstream part of the channel was registered in all runs. In the tests with the short weirs, the measured water surface elevation was also generally found 1.45 cm higher than that observed with longer ones and with a steeper profile over the weir (i.e. higher differences between upstream and downstream water depths, despite of a shorter distance).

These results enrich previous findings on the effects induced by the presence of side weirs on bed morphology (Rosier 2007; Rosier et al. 2009, 2010; Paris et al. 2012; Michelazzo et al. 2016), by extending the analysis also to inclined configurations. It should be noted that, due to the small size of the flume, scale effects affect the results of the physical model: no ripples were registered in any experimental run and bed forms showed slightly three dimensional features. This is in agreement with the results of Williams (1970), who tested the effects of channel width and flow depth on the development of bed forms, showing that similar experimental conditions corresponded with the onset of three dimensional bed forms, without ripples.

3.2. Assessment of the validity of De Marchi's approach

An estimate of the reduction k coefficient was obtained by applying Eq. (1) to the experimental data related to bed deformation, water depth and flow measurements. Figure 4 shows that, although with some scatter, in line with Paris et al. (2012), k is an increasing function of Q_d/Q_1; in this case, it was found by regression analysis that the relationship between these two variables could be expressed as: $k = 1.14 \cdot Q_d/Q_1$ (Figure 4a). By substituting this relation into Eq. (3), it was possible to verify the validity of the De Marchi's assumption even for inclined weir configurations in movable bed conditions, given that energy variations along the lateral weir did not exceed 5% (Figure 4b), i.e. $E_1 \simeq E_2$, independently of crest slope.

It is worth noting that with the approach proposed by Paris et al. (2012), we also obtained some cases in which $E_2 > E_1$, implying an increase in the energy content of the flow along the weir. Obviously, this result would be physically impossible and it derives from the a-priori assumption of energy conservation for fitting the law $k=f(Q_d/Q_1)$; therefore, it seems reasonable to consider that the condition $E_1=E_2$ is a (not strictly achievable) upper limit, rather than an average result, and so one should expect slightly lower k values.

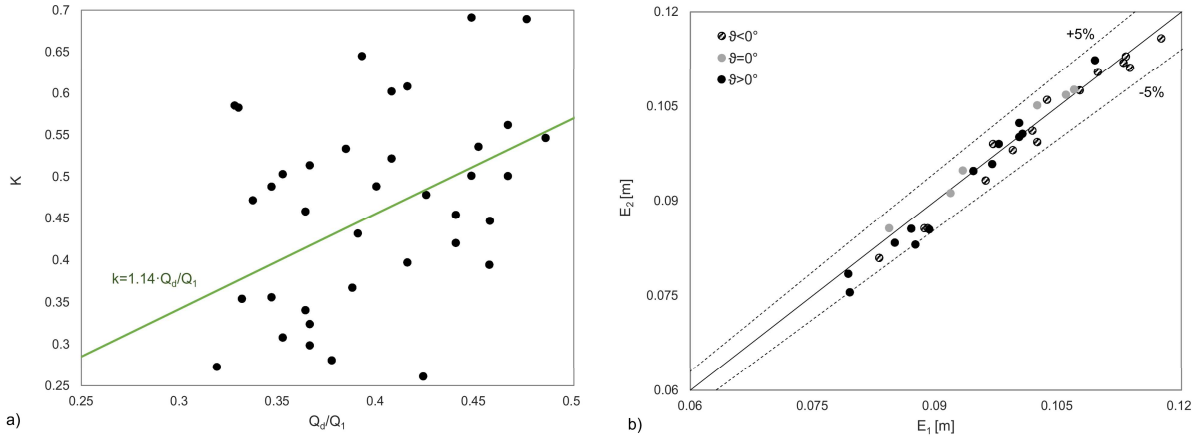

Figure 4. a) Experimental determination of the reduction coefficient k; b) Specific energy at the upstream E_1 and downstream E_2 end of the side weir.

3.3. Analysis of sediment outflow over the side weir

Due to modifications in channel bed morphology induced by the flow withdrawal operated by the side weir and the consequent deposition at the inlet section, in each experimental run it was measured the quantity of sediments leaving the main channel from the lateral structure, as described in Section 2.1.

Figure 5 reports the observed values of the diverted solid discharge as a function of the inclination of the weir crest, for short and long weir configurations. For the highest Q_1 flow rate, the horizontal crested weir was found to release more sediments than the corresponding inclined ones, with q_{sb} tending to be proportional to $cos(\vartheta)$. This behavior can be explained by the flow concentration on a small portion of the crest, occurring especially for the larger inclinations, for which the crest length affected by high flow velocities (able to put the sediment in suspension) is shorter. This result suggests that inclined side weirs can be a suitable option in practical applications where spilled solid flow from the main channel should be avoided or limited to prevent sedimentation, as, for instance, in weirs feeding hydroelectric power plants or detention basins. In some of the runs with inclined crest, the water depth above the higher part of the weir was lower than 3 cm, causing the jet to be affected by surface tension (Novak et al. 1981) in a limited part of the weir.

As a second step, the approach proposed by Michelazzo et al. (2016) for estimating q_{sb} was tested by comparing predicted values to our experimental ones. With the cited method, the predicted sediment transport outflowing from the weir was in the range of 0.22 - 10.22 g/s, with an average of 3.1 g/s, as opposed to the measured one, ranging from 0.04 to 10.89 g/s, with an average of 3.89 g/s; the error in the estimates was found to be independent of weir inclination. These results indicate a good reliability of Michelazzo et al.'s approach for roughly predicting (at least the order of magnitude) the spilled solid discharge even for inclined side weirs configurations.

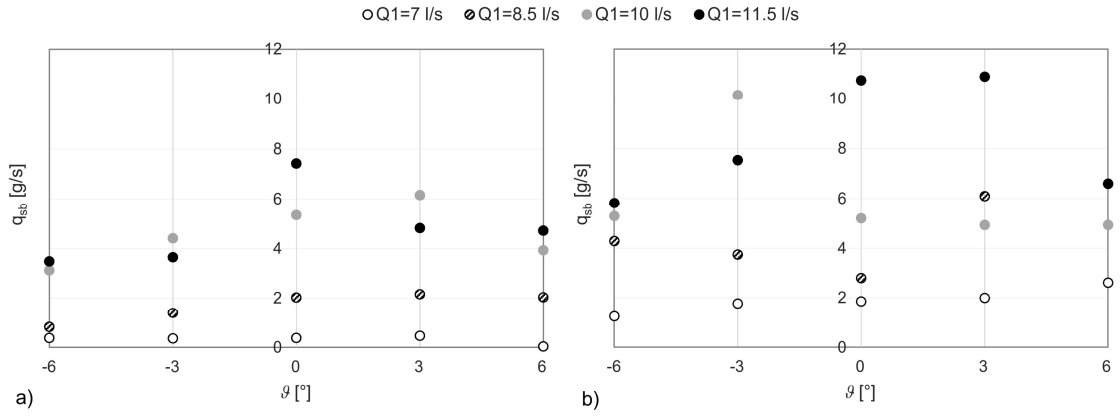

Figure 5. Measured solid discharge outflowing from the side weir, as function of crest angle ϑ and liquid flow in the main channel Q_1: a) weir length L_2=19.5 cm ; b) weir length L_1=34.5 cm.

4. CONCLUSIONS

In this paper the interaction of inclined side weirs with bed load transport phenomena and bed morphology has been studied experimentally, under different subcritical flow conditions and weir lengths and crest slopes. Results indicated that lateral loss of water in the main channel significantly affects the sediment transport capacity, leading to local aggradation and sediment deposition close to the diversion structure. In particular, upward configurations of the side weir were found to limit the scour in the downstream reach of the channel, while producing a prevailing deposition area near and downstream from the weir section, with weir length having some influence on the final modified bed morphology. Inclined weir geometries were also found to be more effective than horizontal ones in limiting the solid discharge leaving the main channel from the diversion structure. Measured solid flow rates were used to analyze the reliability of extending the analytical method proposed by Michelazzo et al. (2016) for horizontal weirs also for inclined geometries, obtaining satisfactory results. Finally, the experimental observations confirmed the validity of De Marchi's assumption even in the case of movable beds and inclined configurations of the side weir.

REFERENCES

Aghayari, F., Honar, T. and Keshavarzi, A. (2009). A study of spatial variation of discharge coefficient in broad-crested inclined side weirs. *Irrigation and Drainage*, 58(2), 246-254.

Bagheri, S., Kabiri-Samani, A.R. and Heidarpour, M. (2014). Discharge coefficient of rectangular sharp-crested side weirs. Part II: Dominguez's method. *Flow Measurement and Instrumentation*, 35, 116-121.

Bagnold, R.A. (1966) An approach to the sediment transport problem from general physics. US Geological Survey, Washington, DC, USA.

Castro-Orgaz, O. and Hager, W.H. (2012). Subcritical side-weir flow at high lateral discharge. *Journal of Hydraulic Engineering*, 138(9), 777-787.

Coleman, G.S. and Smith, D. (1923) The discharging capacity of side weirs. *Proceedings of the Institution of Civil Engineering*, London, Selected Engineering Paper, No. 6.

De Marchi, G. (1934). Saggio di teoria del funzionamento degli stramazzi laterali. *L'Energia Elettrica*, 11, 849-860 (in Italian).

Di Bacco, M., Scorzini, A.R. and Leopardi, M. (2019) On the experimental assessment of De Marchi's discharge coefficient for inclined side weirs: transfer functions for the application of alternative methods. Proceedings of the 38th IAHR World Congress, Panama City, 27-38. ISSN 2521-716X. doi:10.3850/38WC092019-1029.

Hager, W.H. (1987) Lateral outflow over side weirs. *Journal of Hydraulic Engineering*, 113(4), 491-504.

Maranzoni, A., Pilotti, M. and Tomirotti, M. (2017). Experimental and numerical analysis of side weir flows in a converging channel. *Journal of Hydraulic Engineering*, 143(7), 04017009.

May, R.W.P., Bromwich, B.C., Gasowski, Y. and Rickard, C.E. (2003). Hydraulic design of side weirs, Thomas Telford, London, UK.

Michelazzo, G., Minatti, L., Paris, E. and Solari, L. (2016). Side weir flow on a movable bed. *Journal of Hydraulic Engineering*, 142(6), 04016007.

Muslu, Y. (2001) Numerical analysis of lateral weir flow. *Journal of Irrigation and Drainage Engineering*, 127(4), 246-253.

Neary, V.S., Sotiropoulos, F., and Odgaard, A.J. (1999). Three-dimensional numerical model of lateral-intake inflows. *Journal of Hydraulic Engineering*, 125(2), 126-140.

Novak, P., and Cabelka, J. (1981). Models in Hydraulic Engineering. Pitman Publishing, London, UK.

Paris, E., Solari, L. and Bechi, G. (2012). Applicability of the De Marchi hypothesis for side weir flow in the case of movable beds. *Journal of Hydraulic Engineering*, 138(7), 653-656.

Rosier, B. (2007) Interaction of side weir overflow with bed-load transport and bed morphology in a channel. École Polytechnique Fédérale de Lausanne, Laboratoire de Constructions Hydrauliques, Thesis n. 3872.

Rosier, B., Boillat, J.L. and Schleiss, A.J. (2009). Prediction of interaction between a side overflow and bed-load transport in a channel with semi-empirical approaches. *Canadian Journal of Civil Engineering*, 36(11), 1755-1763.

Rosier, B., Boillat, J.L. and Schleiss, A.J. (2010). Semi-empirical model for channel bed evolution due to lateral discharge withdrawal. *Journal of Hydraulic Research*, 48(2), 161-168.

Subramanya, K. and Awasthy, S. (1972) Spatially varied flow over side weirs. *Journal of the Hydraulics Division*, 98(1), 1-10.

Van Rijn, L.C. (1984). Sediment transport, part II: suspended load transport. *Journal of Hydraulic Engineering*, 110(11), 1613-1641.

Wang, Y., Wang, W., Hu, X., and Liu, F. (2018). Experimental and numerical research on trapezoidal sharp-crested side weirs. *Flow Measurement and Instrumentation*, 64, 83-89.

Williams, G.P. (1970). Flume width and water depth effects in sediment-transport experiments. Geological Survey Professional Paper 562-H. US Government Printing Office, Washington, USA.

Westoby, M.J., Brasington, J., Glasser, N.F., Hambrey, M.J. and Reynolds, J.M. (2012). 'Structure-from-Motion' photogrammetry: A low-cost, effective tool for geoscience applications. *Geomorphology*, 179, 300-314.

Wu, C. (2013). Towards linear-time incremental structure from motion. *2013 International Conference on 3D Vision-3DV 2013*, 127-134.